Figure S1

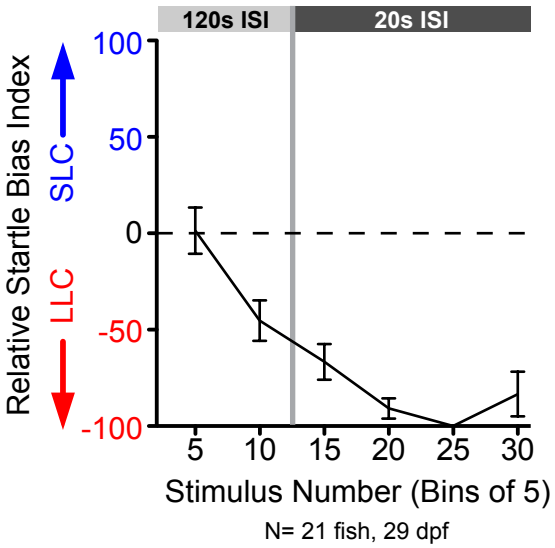

Figure S1. Fish show dynamic change in acoustic response bias at 29 days old, Related to Figure 1.

Average relative startle bias of 29 dpf wild type TLF fish presented with 10 identical 25.9 dB acoustic stimuli at 120 second intervals, followed by 20 identical stimuli at 20 second intervals. N= 21 fish, error bars indicate SEM.

Figure S2

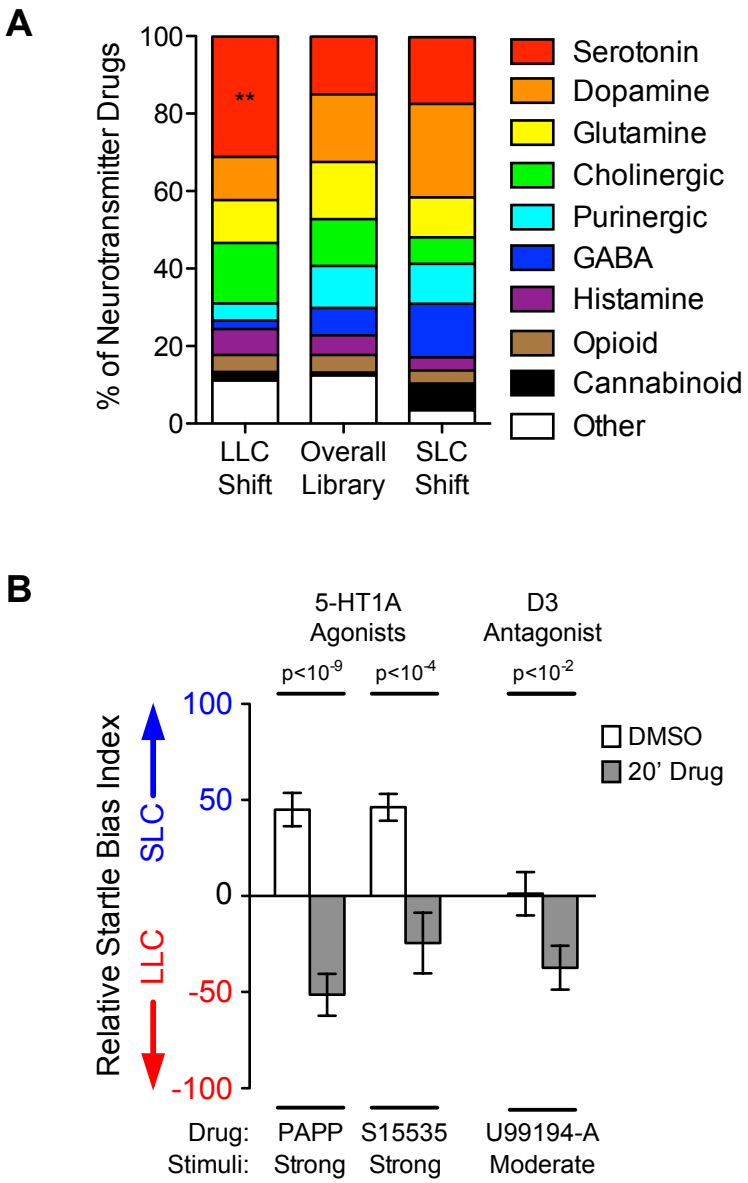

Figure S2: Modulators of serotonin and dopamine neurotransmission shift sensorimotor decision-making, Related to Figure 1.

(A) Summary of drugs annotated to modulate neurotransmission from LOPAC-1280 library that significantly shifted startle bias index toward LLC or SLC behaviors, compared to representation in the library ("Overall Library"). Serotonergic modulators were significantly overrepresented in drugs producing a LLC-shift (**p=0.0087, Fisher Exact Test).
(B) Average relative startle bias of 120-130 hpf larvae treated for 20 min with the 5-HT1A agonists PAPP (N=42 DMSO, 30 10 μM PAPP) or S15535 (N= 46 DMSO, 22 10μM S15535), and the dopamine D3 receptor antagonist U-99194A maleate (N= 45 DMSO, 28 2.5μM U-99194A). Error bars indicate SEM.

Figure S3

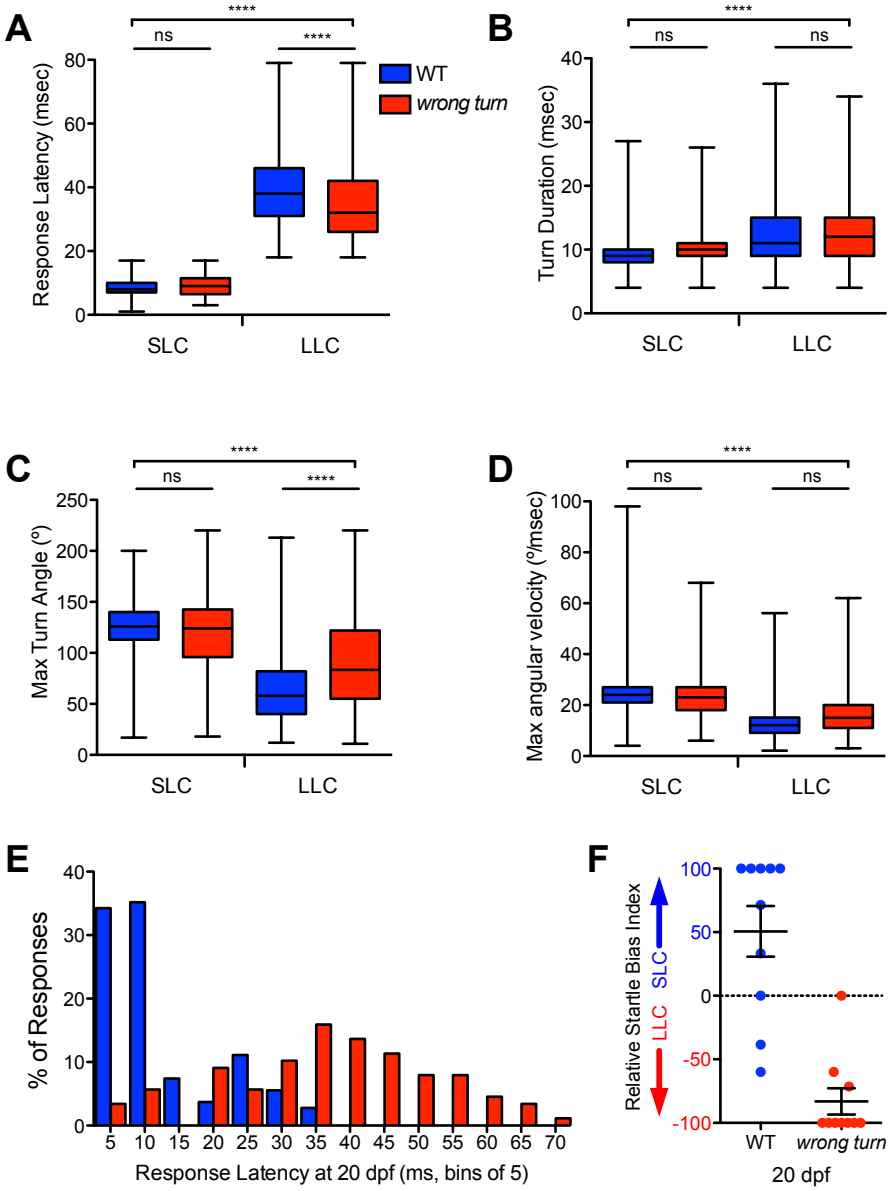

Figure S3: Kinematic comparison of SLC vs LLC behaviors of *wrong turn* mutant larvae and juvenile fish, Related to Figure 2 and Table 1.

(A-D) Average response latency (A), initial turn duration (B), maximal initial turn angle (C), and maximal angular velocity of the initial turn (D) for SLC and LLC behaviors of sibling (blue, N=239 larvae, 3416 responses) and *wrong turn*^{p190} mutant (red, N= 71 larvae, 645 responses) larvae at 5 dpf. Student's t-test was used to compare between sibling and *wrong turn* responses for SLC and LLC behavior, as well as to compare *wrong turn* LLC to sibling SLC response kinematics, with Bonferroni correction for multiple comparisons, ****$p<10^{-4}$.
(E) Histogram of response latency by wild type sibling (blue, N=10) and *wrong turn* mutant (red, N=10) fish to 26 dB acoustic stimuli, aged 20 dpf.
(F) Relative startle bias index of fish tested in (E). Line and error bars indicate mean and SEM. $p<10^{-4}$ for student's t-test.

Figure S4

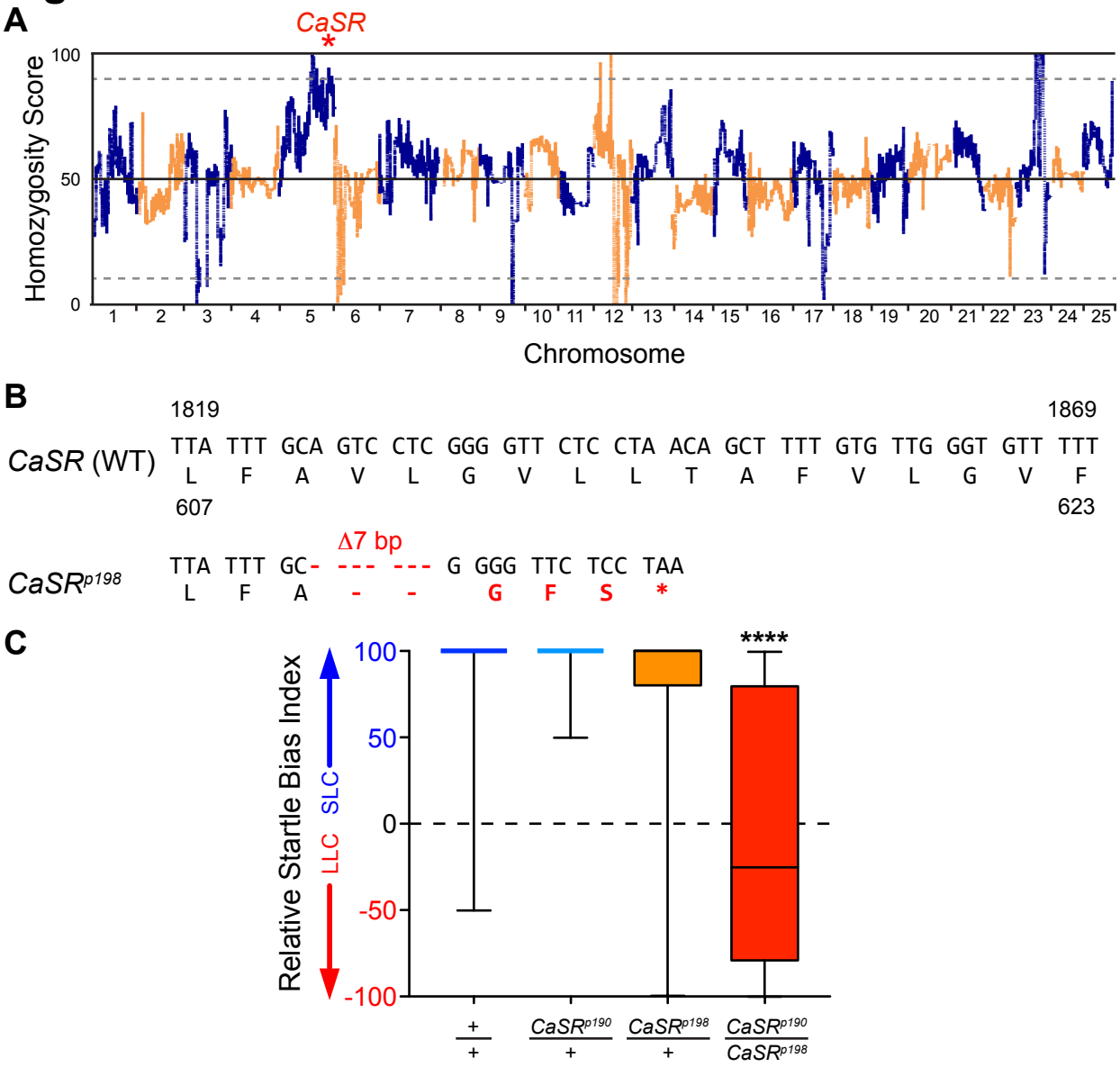

Figure S4: Mapping and validation of *CaSR* mutant alleles, Related to Figure 2.

(A) Plot of homozygosity score across the zebrafish genome for the *wrong turn*^{p190} mutation. Dotted lines mark homozygosity scores of 10% and 90%. The location of *CaSR* (Chromosome 5: 71.19 Mb) within linked SSLP marker region (Chromosome 5: 70.6 – 71.4 Mb) is marked with a red asterisk. Chromosomal locations refer to the Zv9 zebrafish reference genome assembly. Markers on odd numbered chromosomes indicated in blue, even numbered chromosomes in gold.
(B) Sequence of the CRISPR-generated *CaSR*^{p198} allele. Numbers above genomic DNA sequence indicate base number in zebrafish *CaSR* mRNA sequence. Numbers below amino acid sequence indicate position in CaSR protein. Presented sequence is a subset of the 1st transmembrane domain of CaSR.
(C) Relative startle bias indices of 120-130 hpf larvae carrying the *CaSR* alleles indicated, tested with 10 identical 25.9 dB stimuli at 20 second ISI. N= 18 wild type (+/+, dark blue), 20 *CaSR*^{p190}/+ (*wrong turn* allele heterozygote, light blue), 18 *CaSR*^{p198}/+ (CRISPR-generated allele heterozygote, orange), 25 *CaSR*^{p190}/*CaSR*^{p198} (transheterozygote, red). Student's t-test was used to calculate significance vs wild type, ****$p<10^{-4}$ with Bonferroni correction.

Figure S5

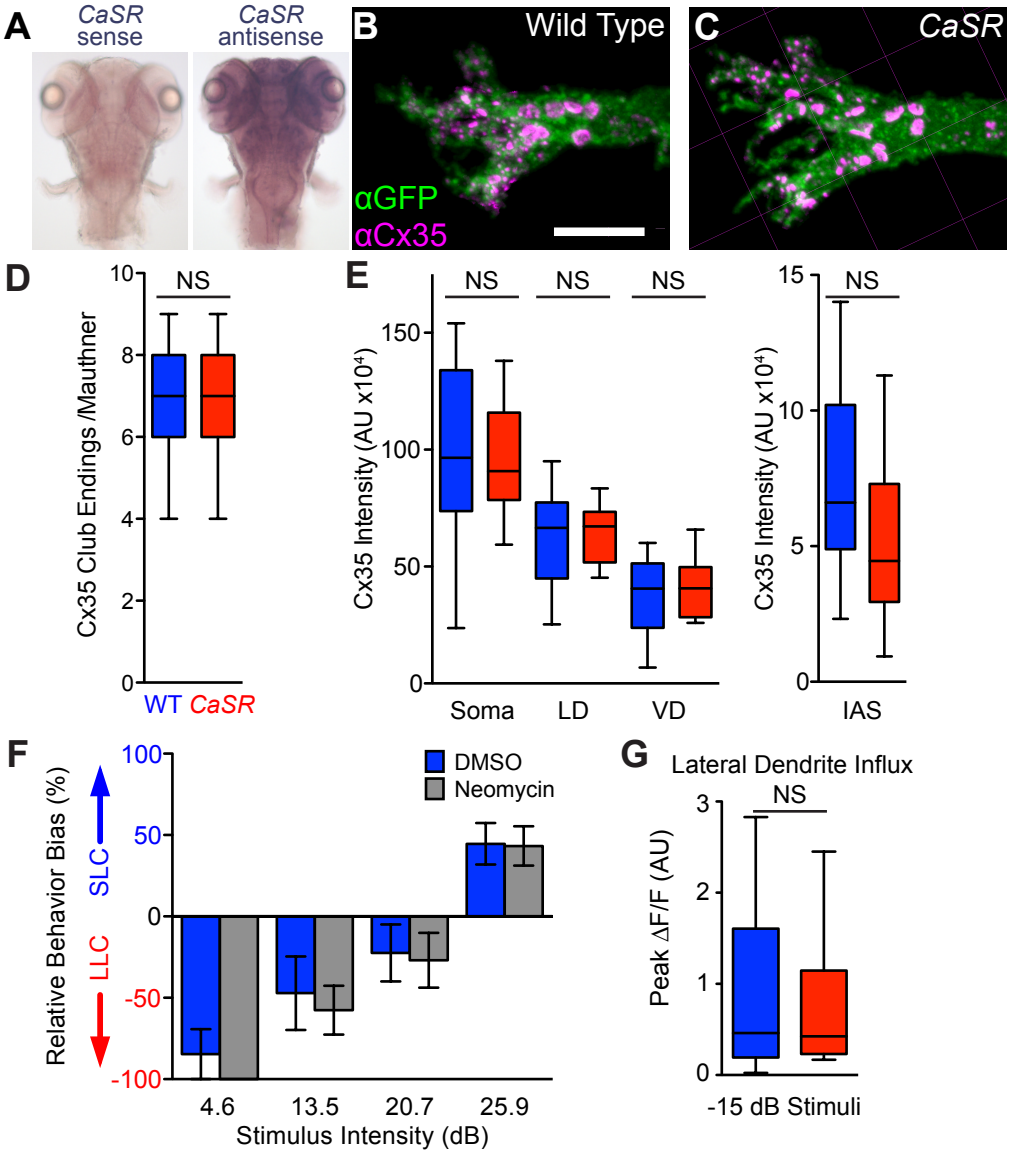

Figure S5: Impact of *CaSR* on Mauthner neuron synapses and synaptic influx, Related to Figure 3.

(A) *CaSR* antisense probe *in situ* hybridization shows broad expression through the brain (104 hpf).
(B-C) Confocal projection images of 144 hpf wild type sibling (A) and *CaSR* mutant Mauthner neuron lateral dendrites. Mauthner neurons labeled with *Tg(hsp70:GAL4FFDMC)130a; Tg(UAS:gap43-citrine)* transgene combination and stained with anti-GFP (αGFP, green) and anti-connexin 35 (αCx35, magenta). Scale bar indicates 10 μm. For clarity, labeling in both channels is shown following thresholding through Imaris software to eliminate non-Mauthner staining.
(D-E) Quantification of αCx35 staining of Mauthner neurons from sibling (blue) and *CaSR* mutant (red) larvae including counts of large Club Ending synapses (C) and total αCx35 intensity on segmented Mauthner neuron surfaces (D). N= 15 wild type siblings and 12 $CaSR^{p190}$ homozygous mutant neurons analyzed (see also Figure 3).
(F) Relative behavioral bias of control larvae (DMSO, blue, N=23) and larvae treated with 40 μM neomycin (grey, N=13) to ablate lateral line sensory neuromasts, 6 dpf.
(G) Peak ΔF/F in the Mauthner lateral dendrite following subthreshold acoustic stimuli (-15 dB) in head-restrained sibling (blue, N=29 stimuli) and $CaSR^{p190}$ mutant (red, N=24 stimuli) larvae expressing GCaMP6s. Statistical comparison by student's t-test (NS, p=0.395).

Figure S6

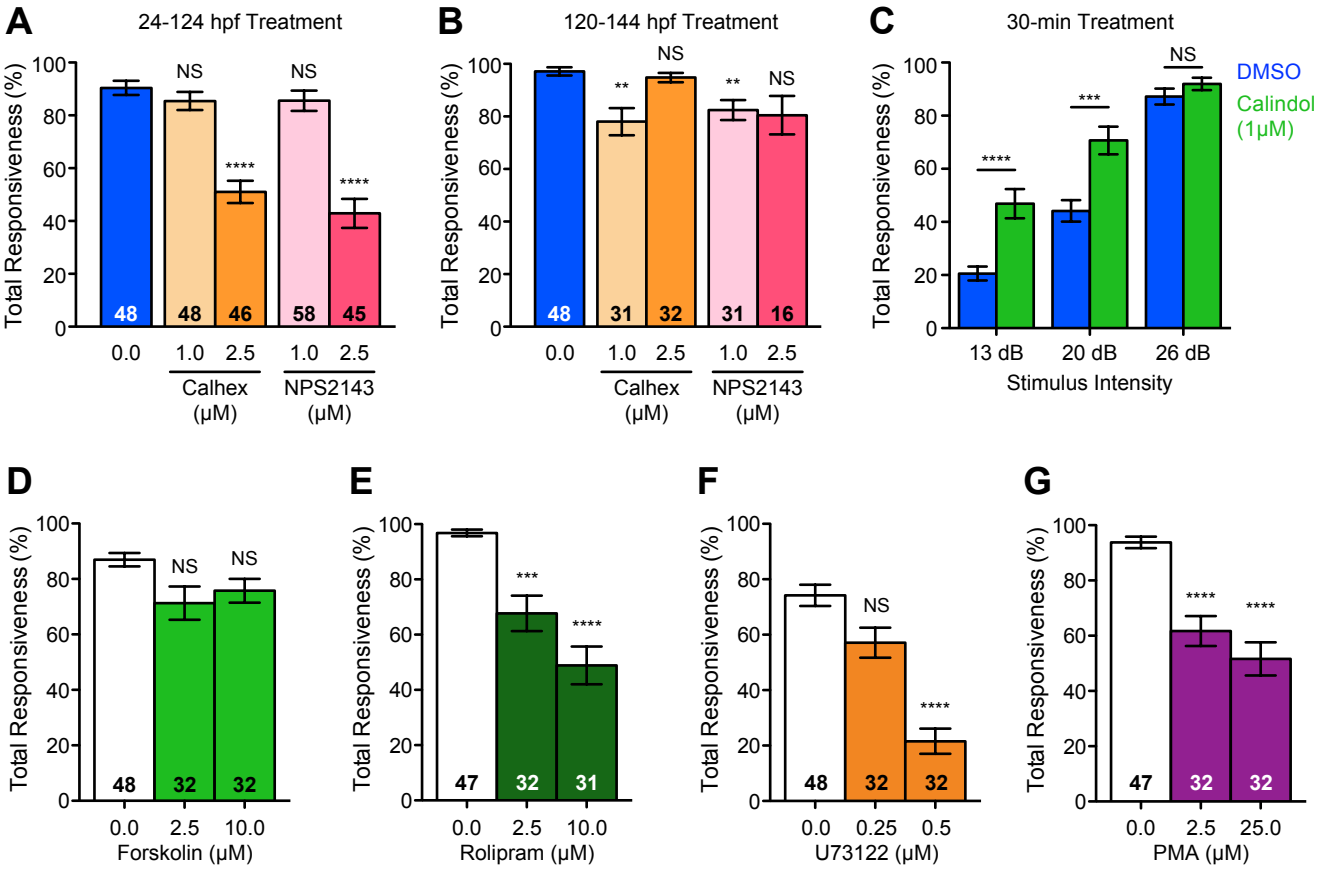

Figure S6: Effect of pharmacological disruption of CaSR pathway components on larval acoustic responsiveness, Related to Figures 4 & 5.

(A) Average responsiveness of larvae to 25.9 dB acoustic stimuli after extended exposure to CaSR antagonists Calhex-231 and NPS2143 for 24-124 hpf.
(B) Average responsiveness of larvae to 25.9 dB acoustic stimuli after exposure to CaSR antagonists Calhex-231 and NPS2143 for 120-144 hpf.
(C) Average responsiveness of larvae to acoustic stimuli after 30 minute acute exposure to CaSR agonist 1 μM Calindol (green, N=32 larvae) vs DMSO control (blue, N=48 larvae).
(D-G) Average responsiveness of 120-150 hpf wild type larvae to 25 dB acoustic stimuli following acute (20 minute) drug treatments.
(D) Treatment with 2.5 μM Rolipram (p=0.00026) and 10.0 μM Rolipram ($p<10^{-6}$).
(E) Treatment with 2.5 μM Forskolin (p=0.058) and 10.0 μM Forskolin (p=0.081).
(F) Treatment with 0.25 μM U73122 (p=0.052) and 0.5 μM U73122 ($p<10^{-12}$).
(G) Treatment with 2.5 μM PMA ($p<10^{-5}$) and 25.0 μM PMA ($p<10^{-6}$).
For all panels, number of larvae tested in each condition are indicated at base of each bar, error bars indicate SEM, **$p<10^{-2}$, ***$p<10^{-3}$, ****$p<10^{-4}$ for Bonferroni-corrected Student's t-test vs. control DMSO treatments.

Figure S7

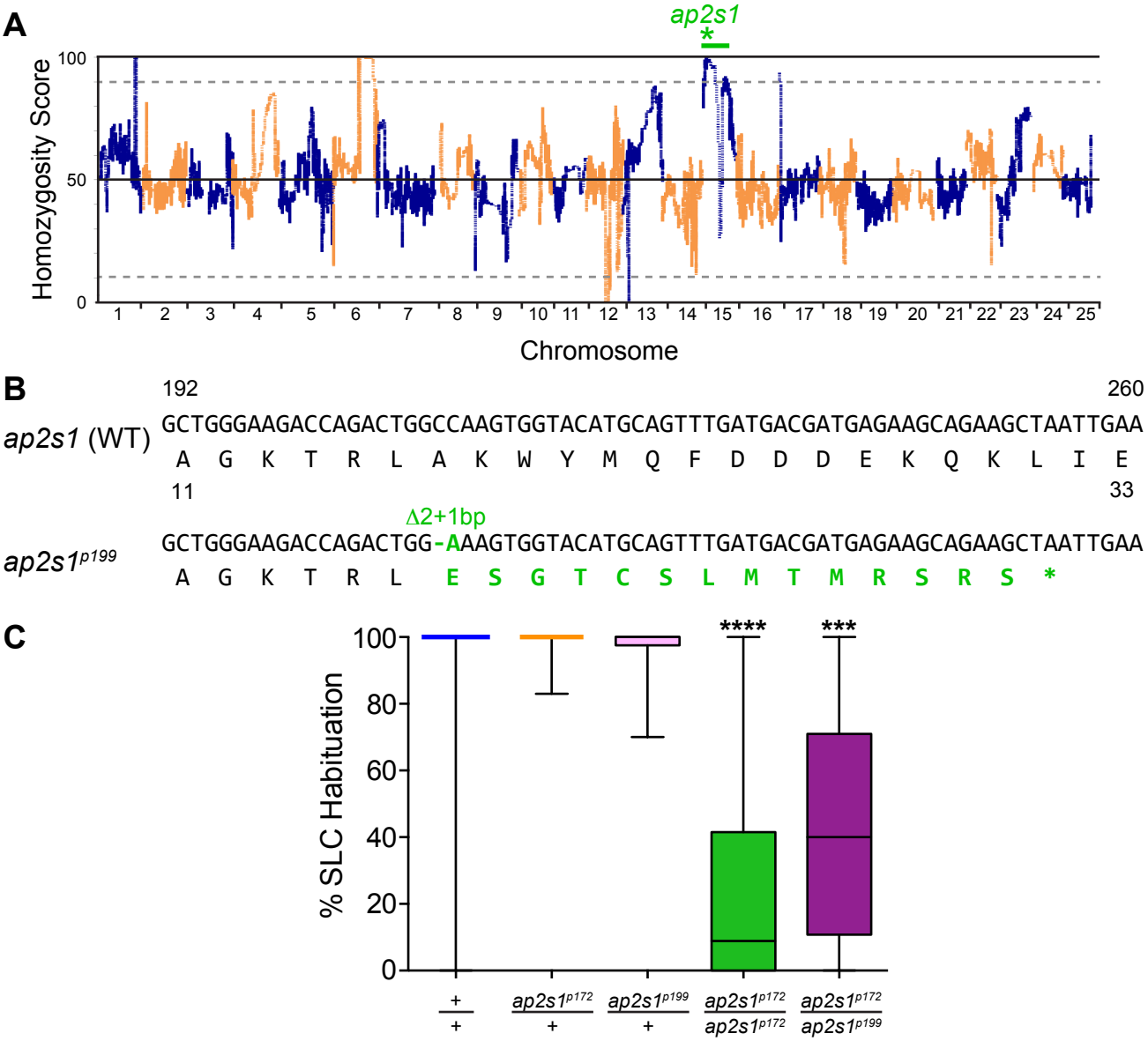

Figure S7: Mapping and validation of *ap2s1* alleles, Related to Figure 6.

(A) Plot of homozygosity score across the zebrafish genome for the *ignorance is bliss*^{p172} mutation. Dotted lines mark homozygosity scores of 10% and 90%. Green bar marks region linked to *ignorance is bliss* phenotype with SSLP markers z4396 (Chromosome 15: 8.46 Mb) and z9189 (Chromosome 15: 33.71 Mb). Green asterisk marks location of *ap2s1* gene (Chromosome 15: 8.9 Mb). Chromosomal locations refer to the Zv9 zebrafish reference genome assembly.
(B) Sequence of the CRISPR-generated *ap2s1*^{p199} allele. Numbers above genomic DNA sequence indicate base number in zebrafish *ap2s1* mRNA sequence. Numbers below amino acid sequence indicate position in AP2σ protein.
(C) Relative SLC habituation of 120-130 hpf larvae carrying the *ap2s1* alleles indicated, tested with 40 identical 25.9 dB stimuli at 20 second ISI (stimuli 1-10) followed by 1 second ISI (stimuli 11-40) to induce habituation. N= 64 wild type (+/+, dark blue), 13 *ap2s1*^{p172}/+ (*ignorance is bliss*^{p172} allele heterozygote, light green), 18 *ap2s1*^{p199}/+ (CRISPR-generated allele heterozygote, pink), 12 *ap2s1*^{p172}/*ap2s1*^{p172} (*ignorance is bliss*^{p172} allele homozygote, green), 12 *ap2s1*^{p172}/*ap2s1*^{p199} (transheterozygote, violet). Student's t-test was used to calculate significance vs wild type, ***$p<10^{-3}$, ****$p<10^{-4}$, with Bonferroni correction.

Table S1: Serotonergic and dopaminergic modulators of acoustic behavioral bias, Related to Figure 1.

Compound	Target(s)	Z_{weak}	Z_{strong}	$Z_{habituation}$	Bias Shift
Serotonergic Modulators					
(±)-8-Hydroxy-DPAT hydrobromide	5-HT1A Receptor Agonist	0.58	-2.78	0.03	LLC
Buspirone hydrochloride	5-HT1A Receptor Agonist	-1.06	-2.53	-0.59	LLC
PAPP	5-HT1A Receptor Agonist	1.28	-2.29	-0.14	LLC
S15535	5-HT1A Receptor Agonist	2.25	-1.98	0.19	Stimulus-dependent
Spiroxatrine	5-HT1A Receptor Agonist	0.47	-1.51	-0.29	LLC
Methiothepin mesylate	5-HT1E, 5-HT1F, 5-HT6 Antagonist	0.74	-0.07	1.57	SLC
Amperozide hydrochloride	Serotonin Receptor Ligand	ND	-0.20	1.69	SLC
Quipazine, 6-nitro-, maleate	Serotonin reuptake inhibitor	0.80	-1.56	1.70	Stimulus-dependent
1-(3-Chlorophenyl) piperazine dihydrochloride	5-HT1 Receptor Agonist	0.68	0.58	1.55	SLC
Cyproheptadine hydrochloride	5-HT2 Receptor Antagonist	1.11	-1.64	-0.93	LLC
Pirenperone	5-HT2 Receptor Antagonist	-0.27	-1.64	-0.70	LLC
Opipramol dihydrochloride	5-HT2 Receptor Antagonist, Sigma 1/2 Agonist	1.26	-2.03	-0.88	LLC
SB 206553 hydrochloride	5-HT2C/5-HT2B Receptor Antagonist	1.15	-1.68	-0.59	LLC
VER-3323 hemifumarate salt	5-HT2C/5-HT2B Receptor Agonist	-0.34	-2.00	0.24	LLC
Ritanserin	5-HT2/5-HT1C Receptor Antagonist	2.10	1.55	2.47	SLC
3-Tropanyl-indole-3-carboxylate hydrochloride	5-HT3 Receptor Antagonist	-1.37	-2.27	0.08	LLC
SB 203186	5-HT4 Receptor Antagonist	2.78	-2.96	-1.09	Stimulus-dependent
SB 204070 hydrochloride	5-HT4 Receptor Antagonist	-0.54	-1.75	-0.10	LLC
Dopaminergic Modulators					
cis-(Z)-Flupenthixol dihydrochloride	Dopamine Antagonist	1.20	0.94	1.56	SLC
1-Phenyl-3-(2-thiazolyl)-2-thiourea	β-Hydroxylase Inhibitor	0.21	1.30	1.67	SLC
R(-)-N-Allylnorapomorphine hydrobromide	Dopamine Agonist	1.22	1.48	1.63	SLC
GBR-12909 dihydrochloride	Dopamine Reuptake Inhibitor	1.86	1.19	2.00	SLC
(±)-Quinpirole dihydrochloride	D2/D3 Receptor Agonist	-1.21	-1.50	-0.69	LLC
A-77636 hydrochloride	D1 Receptor Agonist	-1.38	-2.51	-0.32	LLC
(±)-PPHT hydrochloride	D2 Receptor Agonist	2.35	1.17	2.75	SLC
(±)-Butaclamol hydrochloride	D2, D1 Receptor Antagonist	2.34	1.82	2.33	SLC
Droperidol	D1, D2 Receptor Antagonist	-1.12	-2.30	-0.85	LLC
Pimozide	D2 Receptor Antagonist	-1.35	-2.38	-0.69	LLC
U-99194A maleate	D3 Receptor Antagonist	0.43	-2.40	-0.24	LLC
R-(+)-7-Hydroxy-DPAT hydrobromide	D3 Receptor Agonist	2.49	1.28	1.77	SLC

A Z-score threshold of ±1.5 was used to identify candidate hits, with Z >+1.5 indicating a bias shift toward SLC behavior (blue shading) and Z<-1.5 indicating a shift toward LLC behavior (red shading).

Table S2. Electrophysiological properties of Mauthner neurons, Related to Figure 3.

Parameter	Wild Type (n=6 larvae)	*CaSR*^{p190} Mutant (n=11 larvae)	p-value
Rheobase (nA)	2.5 ± 0.2	2.7 ± 0.2	0.57
$V_{resting}$ (mV)	-79.4 ± 0.4	-79.0 ± 1.1	0.71
R_{in} (MΩ)	9.9 ± 1.1	11.1 ± 1.2	0.50
$V_{Threshold}$ (mV)	-54.6 ± 1.5	-50.0 ± 0.9	0.028

Average ± SEM values for the rheobase, resting potential ($V_{resting}$), input resistance (R_{in}), and action potential threshold ($V_{Threshold}$) of Mauthner neurons of wild type sibling and *CaSR*^{p190} mutant larvae (5-6 dpf) are presented. Two-tailed t-test with Welch's correction for unequal variance was used to determine p-values.

Table S3: PCR primers for molecular cloning and genotyping *CaSR* and *ap2s1* alleles, Related to STAR Methods.

Primers	Forward Sequence	Reverse Sequence
For Genotyping		
CaSR^{p190} dCAPS	AGCTGCGTAGATAGACGGAAA	ACTGGAAGTGCTCGATGATG
CaSR^{p190} KASP	Proprietary	Proprietary
CaSR^{p198}	ACTTTTCTCCACAGATGCCAGT	AAAGCAAAAGAAACGACAGCTC
z26127 SSLP marker	CATCATTTCTGTGCCACTGG	CCGTGATGCTTTTACACCCT
z4299 SSLP marker	AGGAATGCGCTATGGGACGA	CACATCTGCCACTGAACCGG
ap2s1^{p172} dCAPS	GTACTTCTGCATCTGTGTGG	TTAAAGCTGGCTTTTGTCAAATTTG
ap2s1^{p199}	CCAACTTTACCCCAATAAGGTTT	CAGCATGCACCTCTTCAATTAG
z4396 SSLP marker	GGGATTGTGGTTCTCCACGC	AGGCAGCCCTTTCCTAAAGGC
z9189 SSLP marker	TCCAGGTTTGCGTGTGATAG	CCAGTGTGAAACCCGAGAAT
For Cloning		
CaSR CRISPR sgRNA	TAGGCCTTATTTGCAGTCCTCG	AAACCGAGGACTGCAAATAAGG
ap2s1 CRISPR sgRNA	TAGGAAGACCAGACTGGCCAAG	AAACCTTGGCCAGTCTGGTCTT
CaSR cDNA cloning	ATGAGGTTTCATCTGAAGTTTTAC	CCCATCCTTGATCCAATGAC